PAPER *Special Issue on Signals, Systems and Electronics Technology*

Turbo Equalization of GMSK Signals Using Noncoherent Frequency Detection

Tomoya OKADA†, ***Student Member and*** **Yasunori IWANAMI**†a), ***Regular Member***

SUMMARY In this paper, we propose a turbo equalization scheme for GMSK signals with frequency detection. Although the channel is AWGN, there exists severe ISI (Inter-Symbol Interference) in the received signal due to the premodulation Gaussian baseband filter in the transmitter as well as the narrowband IF filter in the receiver. We regard these two filters as a real number inner convolutional encoder. The ISI equalizer for this inner encoder and the outer decoder for a RSC (Recursive Systematic Convolutional) code, are connected through a random (de-)interleaver. These inner and outer decoders generate the reliability values in terms of LLR (Log Likelihood Ratio), using MAP or SOVA algorithm with SISO (soft input and soft output). Moreover iterative decoding with the limitation of LLR values are employed between two decoders to achieve a turbo equalization for GMSK frequency detection. Through computer simulations, the proposed system shows the BER $= 10^{-5}$ at $E_b/N_0 = 8.8$ dB, when we take $BT = 0.6$ (IF filter bandwidth multiplied by symbol duration) with the iteration number of 3. This means 3.1 dB improvement compared with the conventional scheme where the inner ISI equalizer is concatenated with the outer hard decision Viterbi decoder.

key words: *GMSK, ISI, limiter-discriminator detection, iterative equalization*

1. Introduction

Noncoherent L/D (Limiter/Discriminator) detection of digital FM is quite simple to implement and is robust [1]–[6]. The channel, however, is a severe ISI channel due to the baseband premodulation filtering in the transmitter as well as the narrowband IF filtering in the receiver. To compensate for these ISI's and minimize the bit error rate (BER) at the receiver side, decision feedback equalizer (DFE) [7], [8]; or maximum likelihood sequence estimation (MLSE) [1]–[3] (Viterbi Equalizer) has been employed. The SE scheme using the Viterbi algorithm (VA) can be applied successfully, although the VA does not imply maximum likelihood in the strict sense, because the overall channel interference is not purely an additive white Gaussian noise (AWGN). In [2], [3] one of the authors reported a large BER improvement obtained by SE with multiple states trellis for digital FM signals such as GMSK and CPFSK in the case of very narrowband IF filtering with the time-bandwidth products in the range of $BT = 0.5$–0.8. In [9] he also investigated the SOVA decoding [10] for the channel ISI, concatenated with outer two-dimensional parity check codes.

On the other hand, the turbo equalization schemes for BPSK signals were proposed in [11], [12]. In those schemes, the trellis based on outer encoder and the one based on inner ISI encoder derived from the channel tap coefficients of discrete time multipath channel, are found. They are iteratively decoded using two SISO decoders connected through a random (de-)interleaver. It is reported that the BER characteristic obtained is close to the one of no ISI channel. Furthermore turbo equalizers for GMSK signals have been proposed in [13]–[15], but they never use a noncoherent L/D detector, which is simple and robust.

In this paper we have tried to realize a turbo equalization scheme for GMSK signals with noncoherent L/D detection. The channel is AWGN channel, however as stated above, there exists severe ISI in the received signal. We have employed the inner ISI equalizer and the outer RSC decoder, both using MAP (BCJR) [16] (actually Max-Log-MAP) or bidirectional SOVA [17] with SISO. By serially concatenating the inner ISI equalizer with the outer RSC decoder through the feedback of extrinsic LLR, the turbo equalization has been achieved. Also, the existence of click noise at the output of L/D makes the MAP or SOVA decoding less efficient. It becomes a serious problem in the case of iterative decoding. We have adopted threshold devices between two decoders to avoid overestimating output LLR values and solved this problem.

2. Channel Model

Figure 1 and Fig. 2 show the block diagrams of transmitter and receiver respectively. First, the data bits are encoded by the outer RSC encoder and interleaved by a random interleaver. Then, the NRZ pulses are Gaussian baseband-filtered, FM modulated and transmitted to the channel. The channel is a static AWGN channel.

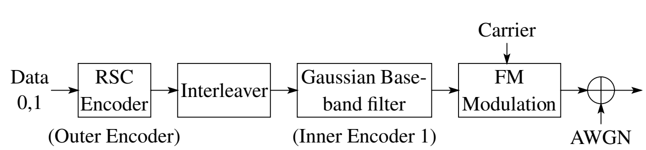

Fig. 1 Transmitter model for coded GMSK.

Manuscript received July 31, 2001.
Manuscript revised October 30, 2001.

†The authors are with the Department of Electrical and Computer Engineering, Nagoya Institute of Technology, Nagoya-shi, 466-8555 Japan.
a) E-mail: iwanami@elcom.nitech.ac.jp

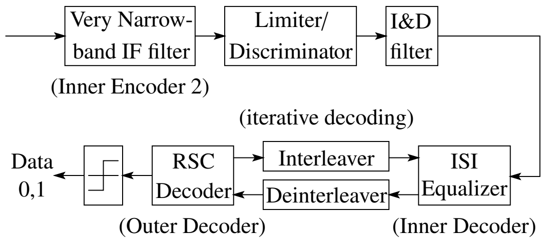

Fig. 2 Received model for coded GMSK.

At the receiver side, a very narrow-band Gaussian IF filter such as $BT = 0.5$–0.8 is introduced. The L/D is used to give an estimate of the signal instantaneous frequency and the output of I&D filter is the detection variable. The output of the Limiter is expressed as

$$y(t) = \cos[\omega_0(t) + \phi(t) + \eta(t)] \tag{1}$$

where ω_0 is the center IF angular frequency, $\phi(t)$ is the IF filtered signal phase and $\eta(t)$ is the phase noise expressed as

$$\eta(t) = \tan^{-1}[\xi(t)/\{\sqrt{2\rho(t)} + \zeta(t)\}] \tag{2}$$

where $\xi(t)$ and $\zeta(t)$ are independent Gaussian processes with zero means and $\rho(t)$ is the time varying signal-to-noise ratio defined in [4] and the probability density function of the phase noise in [4] is given as

$$p(\eta) = \int_0^\infty \frac{x}{\pi} \exp[-(x^2 + \rho(t) - 2x\sqrt{\rho(t)}\cos\eta)]\,dx \qquad |\eta| \le \pi. \tag{3}$$

The output from the I&D filter is given by

$$\begin{aligned} \Delta\Phi &= \phi(T) - \phi(0) + \eta(T) - \eta(0) \\ &= \phi(T) - \phi(0) + [\eta(T) - \eta(0)] \\ &\quad \cdot \mathrm{mod}(2\pi) + 2\pi N(0,T) \end{aligned} \tag{4}$$

where $N(0,T)$ denotes the number of clicks in the interval $(0,T)$ [4]. The ISI equalizer using MAP or SOVA algorithm compensates for the ISI caused by both the Gaussian premodulation baseband filter (inner encoder 1) and the very narrow-band IF filter (inner encoder 2). Here we regard the concatenation of these two filters as a real number convolutional encoder (inner ISI encoder). Any type of IF filter can be used, but we have considered here a Gaussian IF filter given as

$$H(f) = \exp\left\{-a\,(f/f_c)^2\right\} \tag{5}$$

where $f_c = B/2$ and $a = \ln 2/2$ respectively and B is the 3 dB bandwidth. The received signal point spread due to the ISI in the absence of noise, are illustrated in Fig. 3. From Fig. 3 we observe the received signal points are concentrated on 18 symmetrical points (S_0–S_{17}). This follows for the narrow-band Gaussian IF filter since the neighbouring two symbols on each side of the detected symbol affect the detected symbol. Consequently, we need consider 5-bit pattern, but the total $2^5 = 32$ received signal points degenerate into 18 different points due to the symmetry of channel impulse response. Moreover, these 18 points can be approximated as 6 points from R_0 to R_5 in Fig. 3, where the ISI is approximated using the 3-bit pattern. We will follow the 3-bit pattern approximation from now on. The ISI rule is depicted as the 4 states trellis diagram in Fig. 4. The state variables $(U_{k-1}U_kU_{k+1})$ in Fig. 4 mean the past, present and future bits fed to the IF filter. For example, the signal points of R_0 and R_2 are produced from the bite patterns of '111' $(-1-1-1)$ and '010' $(+1-1+1)$ respectively. By using MAP or SOVA algorithm to decode this trellis, we can compensate for the channel ISI and improve the BER. Also by feeding the extrinsic information extracted from the inner ISI decoder to the subsequent outer RSC decoder with SISO, the serial turbo decoding with iterative feedback becomes possible.

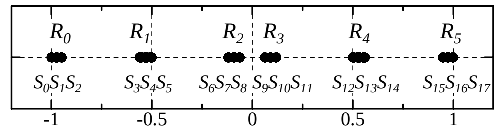

Fig. 3 Received signal point spread due to the ISI introduced by premodulation baseband filter and narrowband IF filter. $(B_bT = 0.25, BT = 0.8)$

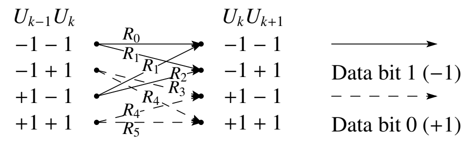

Fig. 4 Trellis representing the ISI rule of channel response.

3. Iterative Equalization

A SISO [18] is shown in Fig. 5 and the iterative equalization is illustrated in Fig. 6. The output sequence $\boldsymbol{y}$ from the I&D filter is fed to the ISI equalizer where $\boldsymbol{y}$ has the length of a trellis with termination. Using the MAP or SOVA decoding scheme, the ISI equalizer generates the LLR $L^E(x_k)$ defined using a posteriori probability (APP) $P(x_k|\boldsymbol{y})$ for the systematic coded bit of the RSC code

$$L^E(x_k) = L^E(x_k|\boldsymbol{y}) = \ln\frac{P(x_k = +1|\boldsymbol{y})}{P(x_k = -1|\boldsymbol{y})}. \tag{6}$$

After de-interleaving, the outer RSC decoder generates the LLR $L^D(u_k)$ on the information bit and the LLR $L^D(x'_k)$ on the systematic coded bit, also by using the MAP or SOVA decoding. The decoder output $L^D(x'_k)$ consists of the extrinsic information and the intrinsic information. The extrinsic information $L^D_e(x'_k)$ is calculated by subtracting the input LLR $L^D_p(x'_k)$ from the

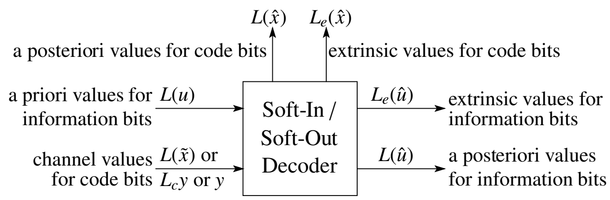

Fig. 5 SISO decoder.

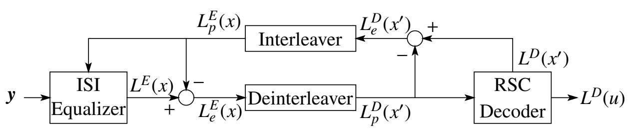

Fig. 6 Block diagram for iterative equalization.

output LLR $L^D(x'_k)$

$$L_e^D(x'_k) = L^D(x'_k) - L_p^D(x'_k). \tag{7}$$

The extrinsic information $L_e^D(x'_k)$ is interleaved and fed back to the ISI equalizer as the priori value and the decoding process is again repeated. This is the first iteration. By utilizing this priori value as the probability weight to each symbol to be decoded, more precise symbol estimation becomes possible. Repeating this iterative operation further improves the BER. Here it is important to say that only the feedback of the quantity corresponding to $L_e^D(x'_k)$ in $L^D(x'_k)$ is needed in order to decrease the correlation between the priori value $L_p^E(x_k)$ to the equalizer and the output LLR $L^E(x_k)$ from the equalizer. For the same reason, the input to the decoder is obtained by subtracting $L_p^E(x_k)$ from the output $L^E(x_k)$ from the ISI equalizer. After several iteration, the hard decision on each information bit is made based on the sign of LLR $L^D(u_k)$.

4. On the MAP and SOVA Algorithms Used in ISI Equalizer and RSC Decoder

The symbol-by-symbol MAP algorithm [16] has been used both for the ISI equalizer and the RSC decoder. On the BER, the MAP algorithm is the optimum decoding algorithm, which gives APP $P(u_k|\boldsymbol{y})$ given the received sequence $\boldsymbol{y}$. The output LLR $L(\hat{u_k})$ for the kth information bit is expressed as

$$L(\hat{u_k}) = \ln \frac{P(u_k = +1|\boldsymbol{y})}{P(u_k = -1|\boldsymbol{y})} = \ln \frac{\sum\limits_{\substack{(s',s)\\ u_k=+1}} P(s', s, \boldsymbol{y})}{\sum\limits_{\substack{(s',s)\\ u_k=-1}} P(s', s, \boldsymbol{y})} \tag{8}$$

where s and s' are the states of the trellis at time k and $k-1$ respectively, and $P(s', s, \boldsymbol{y})$ is the joint probability between the transition from s' to s and $\boldsymbol{y}$. The joint probability $P(s', s, \boldsymbol{y})$ is given by the product of independent probabilities as

$$\begin{aligned} P(s', s, \boldsymbol{y}) &= P(s', y_1^{k-1}) \cdot P(s, y_k|s') \cdot P(y_k^K|s) \\ &= \alpha_{k-1}(s') \cdot \gamma_k(s', s) \cdot \beta_k(s) \end{aligned} \tag{9}$$

where $\alpha_k(s)$, $\beta_k(s)$ are recursively evaluated as

$$\alpha_k(s) = \sum_{s'} \gamma_k(s', s) \cdot \alpha_{k-1}(s') \tag{10}$$

$$\beta_{k-1}(s) = \sum_{s} \gamma_k(s', s) \cdot \beta_k(s). \tag{11}$$

Concerning the branch in the trellis where the transition exists, the transition probability $\gamma_k(s', s)$ for the branch can be expanded as

$$\gamma_k(s', s) = P(y_k|s', s) \cdot P(u_k) \tag{12}$$

where $P(u_k)$ and $P(y_k|s', s)$ denote the priori probability and the transition probability respectively. The difference in calculating the metric between the ISI equalizer and the RSC decoder only exists in the transition probability γ_k of the branch. When defining the signal point value as x_ξ assigned to the transition branch in the MAP equalizer, we can get

$$\gamma_\xi(s', s) = \gamma_\xi^*(s', s) \cdot \exp\left(\frac{1}{2} \cdot x_\xi \cdot L(x_\xi)\right) \tag{13}$$

$$\gamma_\xi^*(s', s) = \exp\left(-\frac{1}{2\sigma^2} \cdot |y_\xi - x_\xi|^2\right) \tag{14}$$

where σ^2 means the noise power of AWGN channel and x_ξ corresponds to each one of R_0–R_5 in Fig. 3. Likewise for the RSC decoder it holds

$$\gamma_k(s', s) = \exp\left(\sum_{\nu=1}^{N}\left(\frac{1}{2}\cdot L(\tilde{x}_k;\nu)\cdot x_{k;\nu}\right) + \frac{1}{2}\cdot u_k \cdot L(u_k)\right) \tag{15}$$

where N is the integer number of denominator of the coding rate, here $N = 2$, and $L(\tilde{x_{k;\nu}})$ is the input LLR given by

$$L(\tilde{x_{k;\nu}}) = L(x_{k;\nu}|y_{k;\nu}) = \ln \frac{P(x_{k;\nu} = +1|y_{k;\nu})}{P(x_{k;\nu} = -1|y_{k;\nu})} \tag{16}$$

where $y_{k;\nu}$ and $x_{k;\nu}$ mean the received signal value and coded signal value respectively. Log-MAP or Max-Log-MAP algorithm is easily obtained from above results.

On the other hand, the SOVA is modified to deliver the reliability value for each bit, based on VA [10]. The decoder selects the path $\boldsymbol{u}$ with the minimum path metric $\mu_{K,\min}$ as the ML path in the same way as VA. The probability of selecting this path is proportional to

$$P(\boldsymbol{u}|\boldsymbol{y}) \sim e^{-\mu_{K,\min}}. \tag{17}$$

Let us denote by $\mu_{k,c}$ the minimum path metric of the paths with the complementary symbol to the ML symbol at time k. If the ML symbol at time k is $+1$, then its complementary symbol is -1. Therefore we can write

$$P(u_k\!=\!+1|\boldsymbol{y})\!\sim\! e^{-\mu_{K,\min}},\quad P(u_k\!=\!-1|\boldsymbol{y})\!\sim\! e^{-\mu_{K,c}}. \tag{18}$$

Then we can rewrite Eq.(8) using SOVA as

$$\ln\frac{P(u_k=+1|\boldsymbol{y})}{P(u_k=-1|\boldsymbol{y})}=\ln\frac{e^{-\mu_{K,\min}}}{e^{-\mu_{K,c}}}=\mu_{K,c}-\mu_{K,\min}. \tag{19}$$

The expression for the path metric of the SOVA was derived by maximizing the joint probability, $P(\boldsymbol{u},\boldsymbol{y})$

$$\begin{aligned} P(\boldsymbol{u},\boldsymbol{y}) &= P(\boldsymbol{u})\cdot P(\boldsymbol{y}|\boldsymbol{u}) \\ &= P(\boldsymbol{u})\cdot\prod_{k=1}^{K}\prod_{\nu=1}^{N}\frac{1}{\sqrt{2\pi}\sigma} \\ &\quad\cdot\exp\left(-\frac{(y_{k,\nu}-x_{k,\nu})^2}{2\sigma^2}\right) \end{aligned} \tag{20}$$

or its logarithm

$$\begin{aligned} \ln P(\boldsymbol{u},\boldsymbol{y}) &= \sum_{k=1}^{K}\ln P(u_k)-\frac{NK}{2}\ln(2\pi) \\ &\quad -NK\ln\sigma-\sum_{k=1}^{K}\sum_{\nu=1}^{N}\frac{(y_{k,\nu}-x_{k,\nu})^2}{2\sigma^2}. \end{aligned} \tag{21}$$

Maximizing $\ln P(\boldsymbol{u},\boldsymbol{y})$ is equivalent to maximizing

$$\sum_{k=1}^{K}\ln P(u_k)-\sum_{k=1}^{K}\sum_{\nu=1}^{N}(y_{k,\nu}-x_{k,\nu})^2 \tag{22}$$

where we do not need to know the actual value of σ^2 as for the maximization of (22) [17]. Consequently, we can define the branch metric and the path metric, assigned to a trellis branch at time k, as

$$\gamma_k^{u_k}=\sum_{\nu=1}^{N}(y_{k,\nu}-x_{k,\nu})^2-\ln P(u_k) \tag{23}$$

$$\mu_k^s=\mu_{k-1}^s+\gamma_k^{u_k}. \tag{24}$$

As the decision is made on a finite length block, the SOVA can be implemented as a bidirectional recursive method with forward and backward recursions [17].

5. Limitation on LLR Value

In the output of L/D, there contain some click noises, especially in the lower E_b/N_0 region, which is peculiar to frequency detection. This is a cause of degrading BER performance. The output from L/D is expressed as

$$V(t)=\frac{d}{dt}[\phi(t)+\eta(t)]. \tag{25}$$

However using the linearization of FM demodulation [3] etc., we can rewrite Eq.(25) as

$$V(t)=\frac{d}{dt}\left[\phi(t)+\xi(t)\cdot\sqrt{N_0\int_{-\infty}^{\infty}|H(f)|^2df}\,\right] \tag{26}$$

where N_0 is the one-sided power spectral density of AWGN. $V(t)$ contains no click noise in (26). This approximation becomes more valid in the high SNR region. Through computer simulations, we have confirmed when there is click noise in the received signal, the output LLR of SISO decoder is overrated and the decoding process cannot function effectively. In this paper, we apply the threshold devices those have certain values, to impose limits on the output LLR values, as shown in Fig. 7.

6. Computer Simulation Results

The simulations are carried out under the following conditions. The transmitted information bits are random and the length of information bits is 512. The outer RSC encoder is shown in Fig. 8, with the rate $R=1/2$ and the memory $M=2$. In order to terminate the trellis, the frame length is selected as 1028 bits. The interleaver applied is a random interleaver. The bandwidth of Gaussian premodulation baseband filter is selected as $B_bT=0.25$ and that of IF filter is selected as $BT=0.6$–1.0. The channel is a static AWGN channel. On the other hand we show the "conventional scheme" in Fig. 9, which means the concatenation of the inner ISI-MAP equalizer and the outer hard decision Viterbi

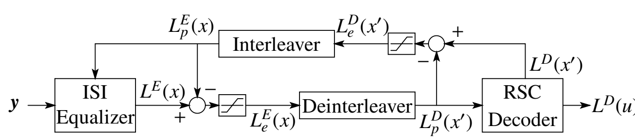

Fig. 7 Block diagram for iterative equalization with the limitation of LLR values.

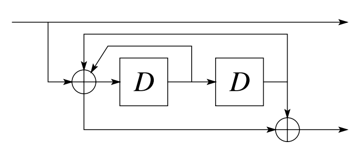

Fig. 8 RSC encoder. ($R=1/2, M=2$)

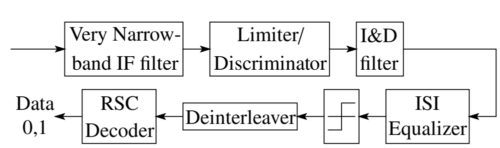

Fig. 9 Conventional receiver model.

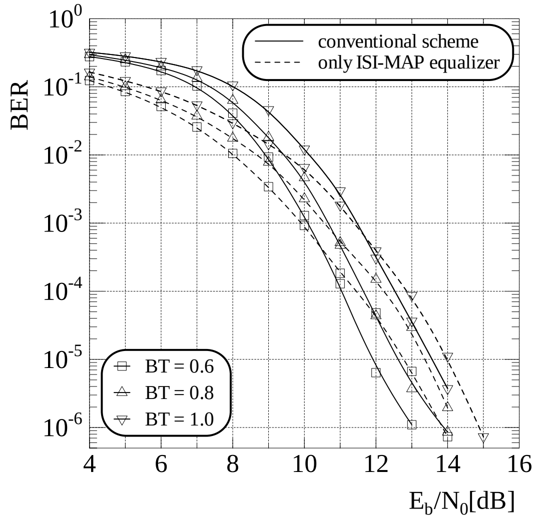

Fig. 10 BER characteristics of GMSK signals using L/D and I&D detection with conventional schemes.

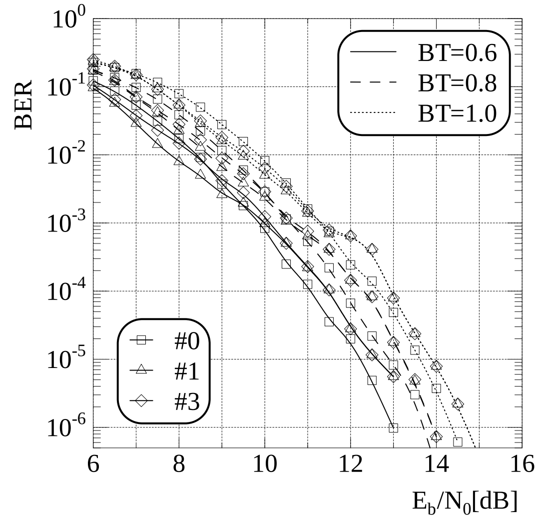

Fig. 12 BER characteristics of turbo equalization scheme for GMSK signals with L/D and I&D detection using SOVA algorithm without LLR limitation.

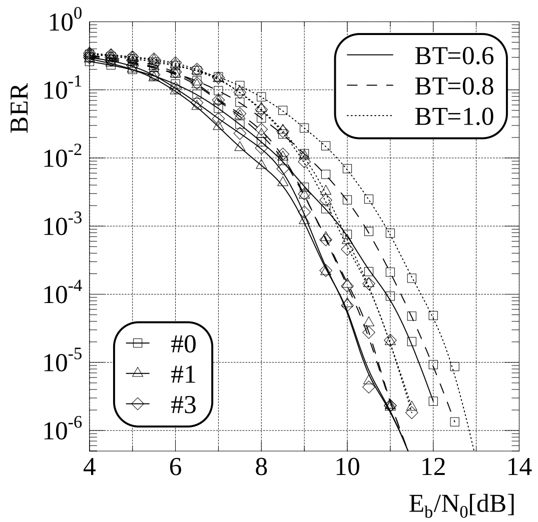

Fig. 11 BER characteristics of turbo equalization scheme for GMSK signals with L/D and I&D detection using Max-Log-MAP algorithm without LLR limitation.

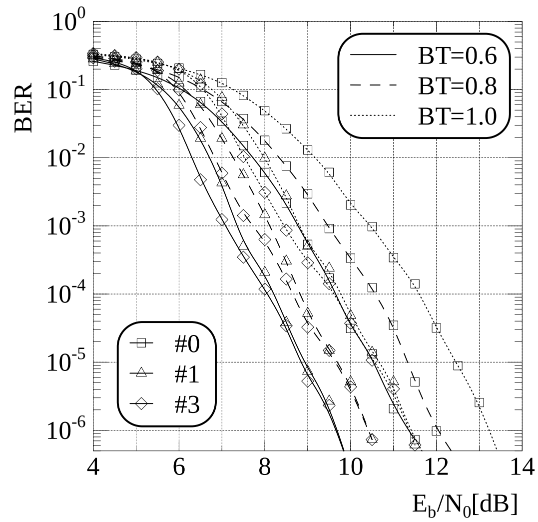

Fig. 13 BER characteristics of turbo equalization scheme for GMSK signals with L/D and I&D detection using Max-Log-MAP algorithm with LLR limitation.

decoder.

Figure 10 shows the BER characteristics of GMSK signals using L/D and I&D detection. The solid line means the conventional scheme, and the broken line means the scheme only using the ISI-MAP equalizer, which means that only the channel ISI is equalized by a MAP equalizer and no outer RSC code is used. Comparing two schemes, coded gain works negatively in lower E_b/N_0 region, but it attains the BER $= 10^{-5}$ at $E_b/N_0 = 11.9$ dB when $BT = 0.6$, meaning 0.9 dB coding gain available due to the outer RSC code.

Figures 11–16 show the BER characteristics of iterative decoding of GMSK signals using L/D and I&D detection. Figures 11, 12 show the BER characteristics with no threshold device (Fig. 6) and Figs. 13, 14 show the BER characteristics when we put the threshold devices between two decoders (Fig. 7). Figures 15, 16 show the BER characteristics under the linearization model.

From Fig. 11, we notice that the scheme attains the BER $= 10^{-5}$ at $E_b/N_0 = 10.4$ dB, when $BT = 0.6$ with 3 iteration. But the effect of iteration number is small and almost 1 iteration is sufficient for the convergence. Besides, from Fig. 12, we see the SOVA algorithm works worse than the Max-Log-MAP algorithm when there is no LLR limitation.

Figures 13, 14 show the BER characteristics when

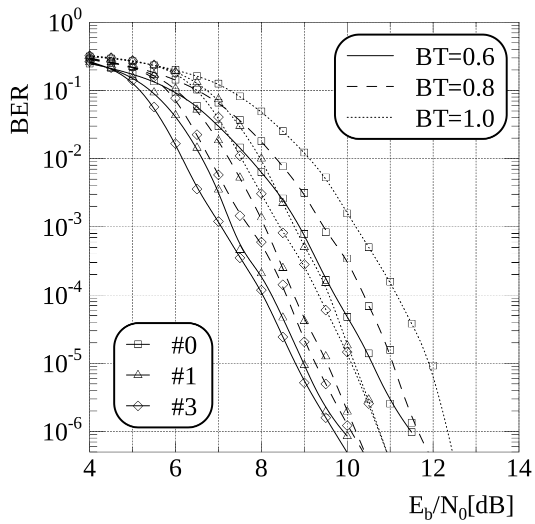

Fig. 14 BER characteristics of turbo equalization scheme for GMSK signals with L/D and I&D detection using SOVA algorithm with LLR limitation.

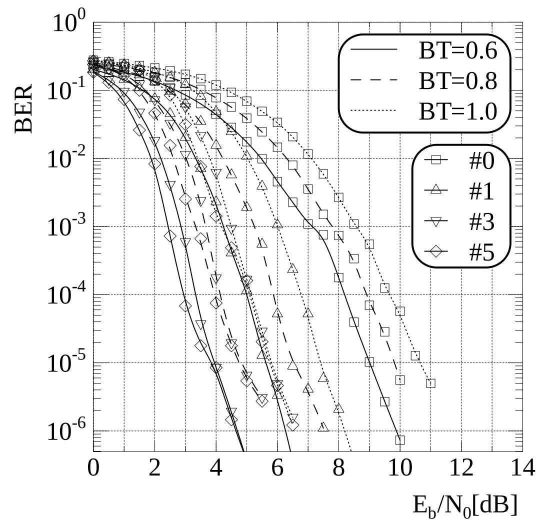

Fig. 16 BER characteristics of Turbo equalization scheme for GMSK signals with L/D and I&D detection under linearization model using SOVA algorithm.

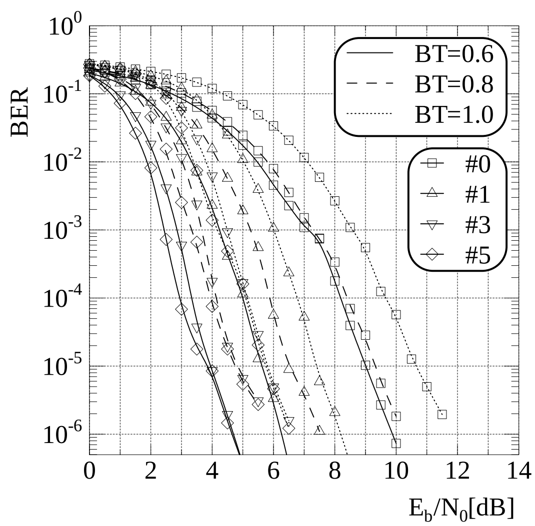

Fig. 15 BER characteristics of turbo equalization scheme for GMSK signals with L/D and I&D detection under linearization model using Max-Log-MAP algorithm.

we put the threshold devices between the two decoders. The threshold value is chosen in consequence of some computer simulations, i.e, $|L_e^E|, |L_e^D| \leq 3$ for Max-Log-MAP decoding and $|L_e^E|, |L_e^D| \leq 1$ for SOVA decoding respectively. In this case the BER is improved effectively compared with the case of no threshold device (Figs. 11, 12) with the iteration number of about 3.

Figures 15, 16 show the BER characteristics under the linearization model, and these are actually impossible to be realized. But by observing Figs. 15, 16, it is obvious that increasing the iteration number to about 5 improves the BER further compared with the real schemes of Figs. 13, 14. Thus for the pure Gaussian noise condition in Figs. 15, 16 in the absence of click noise, we can achieve better BER performance with no limitation on LLR. Accordingly, we might say the need of limitation on LLR comes from the presence of click noise.

Finally, the proposed scheme (Max-Log-MAP or SOVA) shows the BER $= 10^{-5}$ at $E_b/N_0 = 8.8$ dB, when $BT = 0.6$ with 3 iteration (Figs. 13, 14). That is, by introducing the threshold devices, the proposed scheme gains additional 1.6 dB at BER $= 10^{-5}$, and it means 3.1 dB better than the conventional system (Fig. 10).

7. Conclusions

In this paper, we have proposed a novel turbo equalization scheme for GMSK signals with noncoherent Limiter/Discriminator detection. The outer RSC encoder is serially concatenated with the inner ISI encoder for GMSK channel. At the receiver side, the channel ISI is decoded by the inner equalizer using Max-Log-MAP or SOVA algorithm. The iterative decoding has been done between the inner ISI decoder and the outer RSC decoder both using Max-Log-MAP or SOVA algorithm with SISO. Besides, to avoid overrating the output LLR value from SISO decoder, we put the threshold devices between two decoders. As a conclusion we can say the proposed turbo equalizer improves the BER by 3.1 dB at the BER $= 10^{-5}$ for the rate $R = 1/2$ RSC code with the memory $M = 2$, compared with the conventional hard decision Viterbi decoder concatenated with the ISI equalizer.

We have only considered here an AWGN channel, however the proposed scheme is basically applicable to flat Rayleigh or Rice fading channel as well as frequency selective channels. For flat channels, the BER will vary according to the E_b/N_0 variation. But for frequency selective channels the received signal points described in Sect. 2 will be changed in accordance with each channel delay profile and the trellis diagram has to be changed too, hence the channel estimation using pilot symbols etc. will be needed. These are future studies.

Acknowledgement

The authors would like to thank Prof. Emeritus P.H. Wittke, Department of Electrical and Computer Engineering, Queen's University, Kingston, Canada, Dr. R.F. Pawula, Tricel Corporation, San Diego, CA, USA, Prof. Emeritus T. Ikeda and Prof. E. Hayahara, Nagoya Institute of Technology, Nagoya, Japan, for their supports and helpful discussions. This research was supported in part by the scientific fund of Ministry of Education, Culture,Sports, Science and Technology of Japan, the contract No. 13559002.

References

[1] K-S. Chung, "Generalized tamed frequency modulation and its application for mobile radio communication," IEEE J. Sel. Areas Commun., vol.SAC-2, no.4, pp.487–497, July 1984.
[2] Y. Iwanami, "Performance of sequence estimation scheme of narrowband digital FM signals with limiter discriminator detection," IEEE J. Sel. Areas Commun., vol.13, no.2, pp.310–315, Feb. 1995.
[3] Y. Iwanami, "Sequence estimation for digital FM," IEICE Trans. Commun., vol.E84-B, no.6, pp.1613–1621, June 2001.
[4] R.F. Pawula, "On the theory of error rates for narrow-band digital FM," IEEE Trans. Commun., vol.COM-29, no.11, pp.1634–1643, Nov. 1981.
[5] R.F. Pawula, "Refinements to the theory of error rates for narrow-band digital FM," IEEE Trans. Commun., vol.36, no.4, pp.509–513, April 1988.
[6] R.F. Pawula, "Improved performance of coded digital FM," IEEE Trans. Commun., vol.47, no.11, pp.1701–1708, Nov. 1999.
[7] M. Hirono, T. Miki, and K. Murota, "Multilevel decision method for band-limited digital FM with limiter-discrimina tor detection," IEEE J. Sel. Areas Commun., vol.SAC-2, no.4, pp.498–506, July 1984.
[8] F. Adachi and K. Ohno, "Performance analysis of GMSK frequency detection with decision feedback equalization in digital land mobile radio," IEE Proc., vol.135, Pt.F, no.3, pp.199–207, June 1988.
[9] Y. Iwanami, "Sequence estimation scheme of narrowband digital FM signals using limiter-discriminator detection with SOVA," ISITA2000, Honolulu, Hawaii, USA, vol.1, pp.281–284, Nov.2000.
[10] J. Hagenauer and P. Hoeher, "A Viterbi algorithm with soft-decision outputs and its application," Proc. IEEE GLOBECOM89, pp.1680–1686, Dallas, TX, Nov. 1998.
[11] C. Douillard, M. Jézéquel, C. Berrou, A. Picart, P. Didier, and A. Glavieux, "Iterative correction of inter-symbol interference: Turbo-equalization," European Trans. Telecommun., vol.6, pp.507–511, Sept.–Oct. 1995.
[12] G. Bauch, H. Khorram, and J. Hagenauer, "Iterative equalization and decoding in mobile communications systems," 2.EPMCC'97 together with 3.ITG-Fachtagung "Mobile Kommunikation," pp.307–312, VDE/ITG, Sept.–Oct. 1997.
[13] F. Jordan and K.-D. Kammaeyer, "On the application of turbo equalizers in GSM compatible receivers," ISSSE'98, pp.460–464, Sept. 1998.
[14] G. Bauch and V. Franz, "Iterative equalization and decoding for the GSM-system," VTC'98, vol.3, pp.2262–2266, May 1998.
[15] Z. Yang and X. Wang, "Turbo equalization for GMSK signaling over multipath channels based on the gibbs sampler," IEEE J. Sel. Areas Commun., vol.19, no.9, pp.1753–1763, Sept. 2001.
[16] L.R. Bahl, J. Cocke, F. Jelinek, and J. Raviv, "Optimal decoding of linear codes for minimizing symbol error rate," IEEE Trans. Inf. Theory, vol.20, pp.284–287, March 1974.
[17] B. Vucetic and J. Yuan, Turbo codes, principle and applications, Kluwer Academic Publishers, 2000.
[18] J. Hagenauer, E. Offer, and L. Papke, "Iterative decoding of binary block and convolutional codes," IEEE Trans. Inf. Theory, vol.IT-42, no.2, pp.429–445, March 1996.
[19] T. Okada and Y. Iwanami, "Turbo equalization of GMSK signals using limiter-discriminator," Proc. ISSSE'01, Tokyo, pp.424–427, July 2001.

Tomoya Okada received the B.E. degree in electrical and information engineering from the Nagoya Institute of Technology, Nagoya, Japan in 2000. He is currently a master course student of the same institute. His research interests include coded digital FM, and turbo code.

Yasunori Iwanami received the B.E. and M.E. degrees in electrical engineering from the Nagoya Institute of Technology in 1976 and 1978, respectively, and the Ph.D. degree in computer engineering from Tohoku University in 1981. He joined the Department of Electrical Engineering at Nagoya Institute of Technology in 1981 and is currently a Professor of the Department of Electrical and Computer Engineering, Nagoya Institute of Technology. From July 1995 to April 1996 he was a guest researcher in the Department of Electrical Engineering at Queen's University, Ontario, Canada. His current research interests include bandwidth efficient coded modulation, coded digital FM, turbo equalization, space-time signal processing, mobile communication systems and various noise problems. Dr. Iwanami is a member of IEEE and the Society of Information Theory and its Applications (SITA).